COMMUNICATIONS



# MR Molecular Imaging of the Her-2/*neu* Receptor in Breast Cancer Cells Using Targeted Iron Oxide Nanoparticles

Dmitri Artemov,* Noriko Mori, Baasil Okollie, and Zaver M. Bhujwalla

**MR molecular imaging is an exciting new frontier in the biomedical applications of MR. One of the clinically relevant targets is the tyrosine kinase Her-2/neu receptor, which has a significant role in staging and treating breast cancer. In this study Her-2/neu receptors were imaged in a panel of breast cancer cells expressing different numbers of the receptors on the cell membrane. Commercially available streptavidin-conjugated superparamagnetic nanoparticles were used as targeted MR contrast agent. The nanoparticles were directed to receptors prelabeled with a biotinylated monoclonal antibody and generated strong $T_2$ MR contrast in Her-2/neu-expressing cells. The contrast observed in MR images was proportional to the expression level of Her-2/neu receptors determined independently with FACS analysis. In these experiments, iron oxide nanoparticles were attached to the cell surface and were not internalized into the cells, which is a major advantage for in vivo applications of the method. Magn Reson Med 49: 403–408, 2003. © 2003 Wiley-Liss, Inc.**

**Key words: iron oxide nanoparticles; MRI; avidin-biotin system; Her-2/neu receptors**

Noninvasive imaging of cell receptors is a powerful technique that enables early identification of lesions as well as repetitive measurements and more complete coverage, which is not feasible with invasive biopsy techniques. The relatively low concentration of cell receptors in the imaging voxel restricts our choice of imaging modalities to those with the highest sensitivity of detection. Therefore, nuclear imaging techniques such as PET (positron emission tomography) or SPECT (single-photon emission tomography) are most frequently used, although the spatial resolution and volume localization is often a tradeoff with these methods (1). Optical detection is a novel and rapidly progressing technique for imaging of molecular targets in vivo (2). Two alternative approaches have been proposed for in vivo applications: fluorescence imaging of endogenous or exogenous fluorescent markers (3) and imaging of bioluminescence using the luciferase-luciferin system (4). While both approaches provide spectacular images in small animal models, the light penetration depth and light scattering present a serious problem for clinical applications.

MRI is a noninvasive technique routinely used clinically for diagnostic imaging. Intrinsic MR sensitivity is significantly low in comparison with optical and nuclear imaging. To improve it to the level where detection of molecular markers becomes possible, special contrast agents significantly amplifying the MR signals need to be designed. Significant signal amplification can be achieved if the contrast agent is allowed to accumulate in the target cells by passive endocytosis, or by an active transporter system such as a transferrin receptor that shuttles targeted superparamagnetic iron oxide (SPIO) nanoparticles into the cell. These techniques have been successfully used to track cell migration or to detect transgene expression by coupling the transgene expression to the engineered transferrin receptor (5,6). Internalization of the contrast agent by the target cell, essential for these methods, may limit their applications for in vivo studies.

An alternative approach, which does not require internalization, relies on the labeling of extracellular cell surface receptors with a targeted contrast agent. The contrast agent is targeted to a specific receptor by a monoclonal antibody (mAb) or Fab fragments (antigen-binding fragments) of monoclonal antibodies which bind with high affinity to the receptor. Traditionally, gadolinium (Gd)-based contrast agents have been used for MR imaging, as they provide strong positive $T_1$ contrast and a stable complex can be easily formed between Gd and a chelating agent such as DTPA. Since only a limited number of functional groups can be conjugated to the mAb without reducing its binding affinity, the concentration of contrast agent achieved by direct labeling of the mAb is low and frequently not sufficient to generate detectable MR contrast (7). To increase relaxivity, a larger complex such as dendrimer particles (8) or polymerized liposomes with multiple sites for contrast agent labeling can be attached to the mAb. These Gd-based contrast agents were successfully used to image neovasculature in angiogenic tumors with Gd-labeled polymerized liposomes targeted against the $\alpha_v\beta_3$ integrin expressed on neovascular endothelium (9). The large molecular size of these constructs (300–350 nm), however, significantly restricts their delivery and diffusion in tissues.

SPIO microspheres are an alternative contrast agent which generate significant susceptibility changes resulting in strong $T_2$ and $T_2^*$ contrast and, when internalized by cells, enable single-cell MR detection (10). Labeling of inducible E-selectin in human endothelial cells with SPIO-antibody Fab domain conjugates for MR imaging has been previously reported by Kang et al. (11). Human lymphocytes were imaged in vitro using antilymphocytes mAb and biotinylated dextran-magnetite particles (12). The use of small magnetite particles for MRI of tumors is discussed in a review by Go et al. (13). The strong magnetic moment of SPIO particles is the basis for magnetic cell separation. In this technique SPIO Microbeads are directed to cell surface receptors either directly using SPIO-conjugated specific mAb, or indirectly by attachment of SPIO to the cell surface markers prelabeled with primary mAb (14). Following the labeling procedure, cells are separated on a special magnetic column that retains magnetically labeled cells. Viable labeled cells can later be eluted by removing the magnet that generates the magnetic field in the column.

We used components of a standard system developed for magnetic cell separation, for MR imaging of cell receptors. As a target we used the Her-2/neu (c-erb B-2) tyrosine kinase receptor, which is a 185-kD protein (p185) expressed on the surface of breast cancer cells. The Her-2/neu gene was originally identified as an oncogene activated by a point mutation in chemically induced rat neuroblastomas, where it was called *neu* (15). The Her-2/neu protein is overexpressed, usually as a result of HER2/*neu* gene amplification, in approximately 25% of human breast cancers (here and throughout we use capital letters and italic (HER2/*neu*) for the gene and roman (Her-2/neu) for the protein) (16). The expression level of Her-2/neu correlates with poor prognosis for breast and other forms of human cancer (17). Her-2/neu is also a target for immunotherapeutic agents, such as the humanized mAb Herceptin. In HER2/*neu* overexpressing cancers, the success of immunotherapy, targeted against the receptor, is well documented (18). In our experiments we detected expression of Her-2/neu receptors using a two-step labeling protocol as follows: 1) the receptors were prelabeled with biotinylated humanized mAb (Herceptin); and 2) the streptavidin-SPIO $T_2$ MR contrast agent was selectively bound to the prelabeled receptors. Experiments were performed with three established human breast-cancer cell lines which had different expression levels of the Her-2/neu protein.

## MATERIALS AND METHODS

### Cell Lines

We used three human breast cancer cells lines: MCF-7, MDA-MB-231, and AU-565. All cell lines were purchased from the ATCC collection (Manassas, VA) and propagated in culture according to standard protocols. AU-565 is a hormone-independent cell line originally derived from a breast adenocarcinoma. It has an amplified HER2/*neu* oncogene and overexpresses Her-2/neu receptors. AU-565 cells were grown in RPMI-1640 medium supplemented with 4.5 g/L glucose, 10 mM HEPES, 1 mM sodium pyruvate, and 10% fetal bovine serum (FBS). MCF-7 cells, originally derived from an estrogen-dependent mammary adenocarcinoma, were grown in EMEM medium supplemented with 10% FBS. MCF-7 cells express a moderate amount of the Her-2/neu receptor. Hormone-independent breast cancer MDA-MB-231 cells express low numbers of Her-2/neu receptors and were propagated in RPMI-1640 medium with 10% FBS. Cells were grown at 37°C in a humidified atmosphere with 5% $CO_2$; all media contained a mixture of antibiotics (100 U/mL penicillin and 0.1 mg/mL streptomycin). To protect surface proteins for MRI and FACS (flow cytometry analysis) experiments, cells were harvested from the flasks using enzyme-free cell dissociating buffer (Invitrogen, Carlsbad, CA) for up to 30 min at room temperature.

### Biotinylated Antibody

To recognize the extracellular domain of the human Her-2/neu receptor, we used the humanized monoclonal anti-Her-2/neu antibody Herceptin. To enable attachment of streptavidin-SPIO conjugates to the mAb, Herceptin was biotinylated according to a standard protein modification protocol (19). Briefly, Herceptin (gift from Genentech, San Francisco, CA) was prepared in PBS at a concentration of 5 mg/mL and EZ-Link Sulfo-NHS-LC Biotinylation kit (Pierce, Rockford, IL) was used to attach sulfo-NHS-LC-Biotin groups to primary amines of the mAb with a spacer arm of 22.4 Å. Conjugated mAb were separated from low-molecular weight compounds including toxic preservatives, with a dextran desalting column (Pierce). The ratio of biotin/antibody was determined with an HABA colorimetric assay according to the manufacturer's protocol (measured concentration was 5–7 biotins per antibody).

### SPIO Imaging Agent

MACS Streptavidin Microbeads (Miltenyi Biotec, Auburn, CA) were used as a targeted $T_2$ contrast agent. These 50 nm diameter nanoparticles contain a SPIO core coated with a polysaccharide layer (55–59% iron oxide w/w) and are conjugated to streptavidin molecules to provide specific binding to biotinylated compounds.

### Flow Cytometry Analysis

AU-565, MCF-7, and MDA-MB-231 cells were analyzed for the expression of Her-2/neu receptors using biotinylated Herceptin as the primary mAb. A conjugate of streptavidin with fluorescein (Streptavidin-FITC; Molecular Probes, Eugene, OR) was used for fluorescent labeling of the cells. Nonspecific biotinylated antibodies were used in the control studies. Cells were harvested as described earlier and $10^6$ cells were prelabeled with primary mAb (50 μg/mL in 0.5% BSA in 1× PBS for 30 min at room temperature). After extensive washing cells were stained with streptavidin-FITC (20 μg/mL in PBS, 5 min at room temperature). All data were acquired with a FACScan flow cytometer (Becton Dickinson, San Diego, CA). Acquisition parameters were optimized for detection of FITC fluorophore (excitation at 488 nm with an argon laser and detection above 505 nm) (20). Ten thousand events were counted for each cell type. The expression level of the receptor was evaluated using a reference sample consisting of biotinylated microspheres (2 μm diameter, binding capacity 2.3 μg/mg; Polysciences, Warrington, PA) probed with the same streptavidin-FITC conjugate as the cells.

Department of Radiology, Johns Hopkins University School of Medicine, Baltimore, Maryland.

Grant sponsor: NIH; Grant number: P20 CA86346; Grant sponsor: S.G. Komen award; Grant number: IMG 0100775.

*Correspondence to: Dmitri Artemov, Johns Hopkins University School of Medicine, 720 Rutland Avenue, 217 Traylor Building, Baltimore, MD 21205.

Received 19 July 2002; revised 25 September 2002; accepted 1 November 2002.

DOI 10.1002/mrm.10406
Published online in Wiley InterScience (www.interscience.wiley.com).

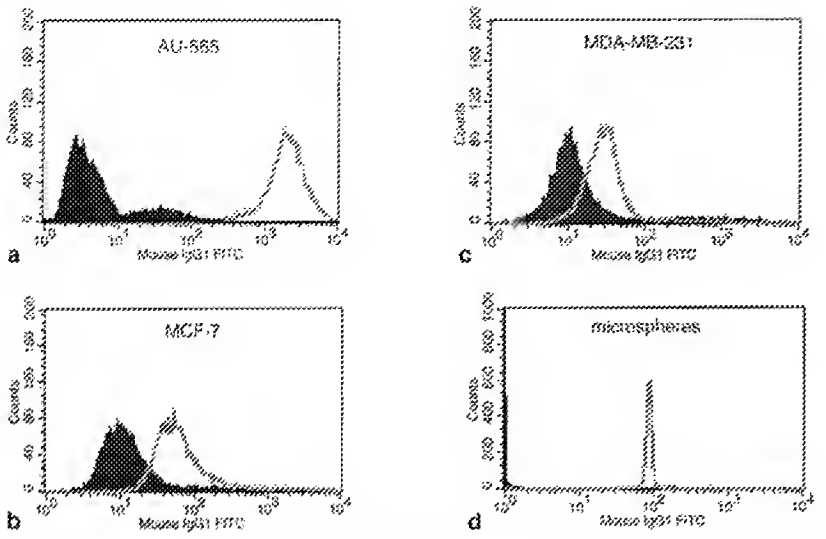


FIG. 1. FACS analysis of Her-2/neu expression for a panel of breast cancer cells. a: AU-565. b: MCF-7. c: MDA-MB-231. All cell lines show detectable expression levels of Her-2/neu. AU-565 cells have the highest expression level and MDA-MB-231 the lowest level. d: Fluorescence from reference microspheres, labeled with the same fluorescent marker, fluorescein isothiocyanate (FITC), as breast cancer cells.

### MRI

For in vitro MR studies, cells were harvested and prelabeled with biotinylated Herceptin as described above. After extensive washing, cells were incubated with streptavidin SPIO Microbeads for 15 min at 4°C in 100 mL labeling buffer containing 10 mL of MACS Streptavidin Microbeads, as recommended in the manual. Control cells were incubated with a nonspecific biotinylated antibody and with MACS Streptavidin Microbeads. After washing, cells were fixed with 2% paraformaldehyde in PBS and $10^7$ cells were embedded in 50 μL of soft agarose gel as a layer in a 5 mm NMR tube. The three different cell lines were placed in the 5 mm NMR tube as three separate layers using agarose gel spacers. The gel consisted of Type IX ultralow gelling temperature agarose (Sigma, St. Louis, MO) prepared as a 3% solution in PBS buffer. A reference sample containing different concentrations of biotinylated microspheres (2 μm diameter, binding capacity 2.3 μg/mg; Polysciences) labeled with MACS Streptavidin Microbeads was similarly prepared. Four layers of 30 μL agarose mixed with 0, 0.25, 1, and 4 μL microspheres were embedded in a separate 5 mm NMR tube. The concentration of binding sites in the layers was 0, $5 \cdot 10^9$, $2 \cdot 10^{10}$, and $8 \cdot 10^{10}$ biotins/μL correspondingly.

MR images of the samples were obtained on an Omega-400 spectrometer (Omega, GE/Bruker, Billerica, MA) equipped with a microimaging system. $T_2$-weighted images were acquired using a 2D spin-echo imaging pulse sequence and a 5 mm proton MR imaging probe (GE/Bruker). For $T_1$ imaging, a spin-echo sequence was used with a magnetization presaturation composite pulse preparation, followed by a recovery delay at each phase-encoding step to reduce potential steady-state effects of conventional spin-echo acquisition with short repetition time. $T_2^*$-weighted imaging was performed with a standard spoiled gradient-recall echo pulse sequence. All experiments were performed with a slice thickness of 1 mm, field of view 24 mm, and in-plane resolution 94 μm (interpolated for the phase-encoding dimension). Pixel-by-pixel relaxation maps were reconstructed from a series of $T_1$, $T_2$, or $T_2^*$-weighted images using a nonlinear two-parameter Powell fitting procedure programmed with IDL (Research Systems, Boulder, CO).

## RESULTS

### Her-2/neu Receptor Expression in Model Cell Systems

Expression of Her-2/neu receptors in MCF-7, AU-565, and MDA-MB-231 cells growing in culture at <70% confluency was detected with FACS analysis. Data shown in Fig. 1 demonstrate a significant shift of fluorescence intensity for all breast cancer cell lines probed with the specific



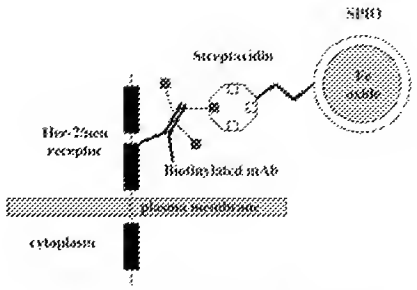


FIG. 2. Schematic representation of the labeling of Her-2/neu expressing cells with targeted SPIO Microbeads using the biotin-streptavidin linker.

antibody. Expression levels of Her-2/neu were quantified using fluorescence of standard calibrated microspheres (Fig. 1d). The estimated number of biotin groups was $1.2 \cdot 10^5$ per microsphere. The estimated number of Her-2/neu receptors available for binding of biotinylated Herceptin per cell was $2.7 \cdot 10^6$ for AU-565, $8.9 \cdot 10^4$ for MCF-7, and $4 \cdot 10^4$ for MDA-MB-231 (a factor of 6, reflecting the number of biotins per Herceptin molecule, was included in the calculations).

### MRI Detection of the Her-2/neu Receptor in Cell Samples

A schematic diagram of the cell labeling procedure using the SPIO contrast agent targeted to biotinylated primary mAb that recognizes cell surface receptors is shown in Fig. 2. $T_2$ images of control and Herceptin-treated breast cancer cells as well as $T_1$, $T_2$, and $T_2^*$-weighted images of a reference sample prepared with biotinylated microspheres are

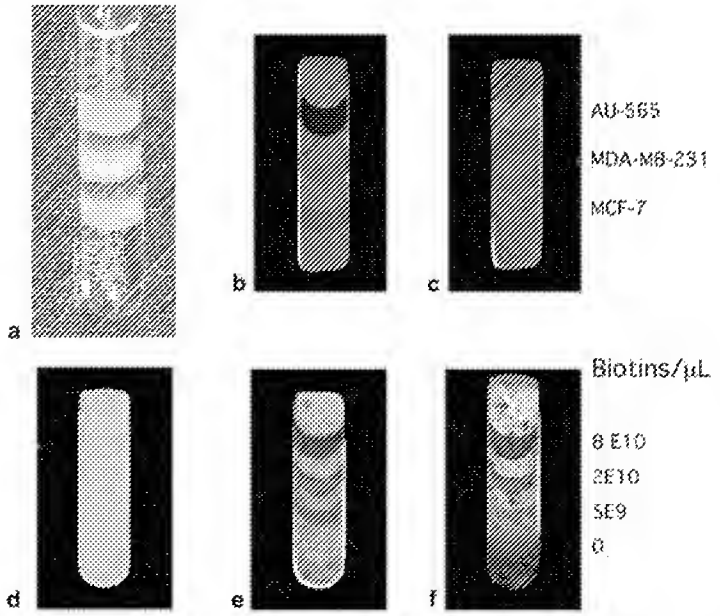


FIG. 3. MR images of breast cancer cells and reference microspheres samples. a–c: The layout and MR images of cell samples consisting of layers of AU-565, MDA-MB-231, and MCF-7 cells embedded in agarose gel in a 5 mm NMR tube. Cells were pretargeted with biotinylated Herceptin and a nonspecific biotinylated mAb (negative control) and probed with streptavidin SPIO Microbeads. $T_2$ maps of the cell samples were reconstructed from eight $T_2$-weighted images acquired with RD of 8 s and TE in the range 20–250 ms. A $T_2$ map of a cell sample probed with Herceptin is shown in b and the control cell sample treated with a nonspecific biotinylated mAb is shown in c. d–f: Display $T_1$, $T_2$, and $T_2^*$ MR maps of the reference sample prepared with biotinylated microspheres labeled with streptavidin SPIO Microbeads. Concentrations of biotin-labeled binding sites in the layers are shown in the image. The $T_1$ map of the sample shown in d was reconstructed from eight saturation recovery images with recovery delays in the range of 100 ms to 5 s. The $T_2$ map shown in e was acquired as in b. $T_2^*$ map of the reference sample (f) was acquired with gradient echo imaging with TE in the range of 10–200 ms.

shown in Fig. 3. A photograph of the cell layers embedded in agarose gel in a 5 mm NMR tube is also shown in the figure. Strong negative $T_2$ contrast was detected in all cell lines probed with a specific Herceptin mAb. Background contrast was not detected in a control sample of cells treated with nonspecific mAb.

As seen from images of the reference sample, the contrast agent produced a very weak $T_1$ contrast (Fig. 3d). $T_2^*$ contrast did not provide significantly more sensitivity than $T_2$ contrast and $T_2^*$ images had substantial inhomogeneity artifacts, which spoiled image quality (Fig. 3f).

## DISCUSSION

A new method for noninvasive imaging of Her-2/neu receptors was tested in different cellular and artificial systems and was shown to provide high sensitivity, with the lower limit of detection in the range of $5 \cdot 10^4$ receptors per cell. This compares favorably with typical expression levels of Her-2/neu receptor in clinical cases of breast cancer, where levels range from $10^5$ to $4.5 \cdot 10^6$ per cell (15,16,21). The method is based on a two-component, SPIO-based targeted contrast agent. Streptavidin-SPIO Microbeads are commercially available, as are the monoclonal antibodies used in the experiments. Biotinylation of the primary mAb is a straightforward procedure that can be performed with commercial kits using standard laboratory techniques and equipment. A possible modification of the system may include three-step labeling, where receptors are pretargeted with biotinylated mAb probed by avidin and then by biotinylated SPIO particles. Using the biotinylated agent at the last step is advantageous, as its molecular weight can be kept low, which improves delivery and clearance of the agent. This is especially important for radioimmunotherapy where rapid clearance of the radioactive ligand contributes to the efficiency of the treatment (22). From our experimental results it appears that $T_2$-weighted spin-echo imaging is the optimal MR method of detection, which provides an efficient negative contrast in MR images and removes artifacts due to local gradients of the magnetic field present in $T_2^*$ maps. $T_1$ contrast generated by SPIO particles was not efficient at the high field (9 T) used in our experiments. In our experiments cells were fixed in a paraformaldehyde solution immediately after the labeling step. This prevented internalization of the antibody with the attached SPIO particle by the viable cells and stabilized the structure of the complex. Paraformaldehyde fixation was required since MRI, which was performed without perfusing cells with medium, might have resulted in cell death and lysis. For in vivo studies, internalization of the mAb attached to the cell surface receptors is an important issue which has to be addressed for optimizing the labeling and imaging protocol. Interestingly, it was demonstrated that the internalized contrast agent may still provide effective contrast for MR imaging (6,10).

To quantify the $T_2$ contrast generated by the contrast agent, we compared changes in $T_2$ relaxation rates determined as $\Delta(1/T_2) = (1/T_2)_0 - (1/T_2)_{\text{postcontrast}}$ for samples with known concentration of binding sites for the contrast agent. Scatter plot analysis of $\Delta(1/T_2)$ as a function of the receptor density is shown in Fig. 4 for the breast cancer

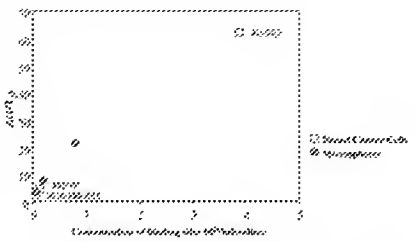

FIG. 4. $T_2$ relaxation rates for breast cancer cells and reference microspheres plotted as a function of binding sites available for labeling with the contrast agent.

cell lines and for different concentrations of biotinylated microspheres used in the reference sample.

Analysis of relaxation properties of SPIO contrast agent demonstrates a positive trend in $(1/T_2)$ relaxation rate with increased concentration of the contrast agent. The curve also suggests a linear dependence of the parameters in agreement with the results reported in (23,24). At this point the linear dependence cannot be proven because of missing data points corresponding to intermediate levels of Her-2/neu expression. A breast cancer cell line with an intermediate level of Her-2/neu is currently unavailable to us. A more complex concentration dependence of relaxation rates was reported by Tanimoto et al. (25) when clustering of SPIO particles, as in Kupffer cells in the liver, occurred. In these studies a special phantom prepared from 1% agar gel with Sephadex beads was used and no changes in $(1/T_2)$ rate were detected with increasing iron concentrations in the range of 0–1.0 mM (25). In our experiments the contrast agent was also localized in compact areas on the surface of cancers cells and/or biotinylated microbeads. The $(1/T_2)$ relaxation rates, however, increased practically linearly with increasing number of SPIO binding sites, as seen from Fig. 4, resembling the relaxation properties of a phantom with uniformly distributed SPIO particles (25). Linear dependence of $(1/T_2)$ relaxation rate on SPIO concentrations is an important advantage of $T_2$ MRI for detection of cells labeled with SPIO particles targeted to cell surface receptors.

Our method does not utilize any explicit amplification strategy but still provides high sensitivity of detection, comparable with methods based on contrast accumulation by internalization into the cell. Labeling of an extracellular target is an important advantage for the in vivo application of the method because of the lower probability of modulating cell physiology. This is especially important for noninvasive MR reporter systems where one can design a nonfunctional receptor expressed under control of the promoter of a target gene (26). The tecbnique also has significant potential for screening endogenous receptor expression in cancers using noninvasive MRI. This approach could be useful for cancer diagnosis and for monitoring tumor therapy targeted against specific receptors. Several issues, however, have to be addressed before the method can be applied clinically. One major potential problem for



in vivo application of the method is the poor delivery of high-molecular weight compounds to the solid tumor interstitium. In our system, the molecular diameter of an SPIO particle of 50 nm corresponds to a molecular weight in the range of 40–50 MD. To improve delivery, the design of novel molecular probes with high relaxivity and small molecular size is essential. A good example of recent advances in this direction is the use of magnetic dendrimers which can provide high relaxivity while maintaining a relatively small molecular size (27,28). Another problem is the potentially harmful immune response of the host to the large amount of antibody and macromolecular imaging agent needed for MR visualization of a receptor. Again, the development of novel, more efficient imaging reagents will reduce the contrast dose required for receptor-specific MRI, thus minimizing the possibility of an immune response.

## ACKNOWLEDGMENTS

We thank S. Stanislavov for assistance with preparing the samples and Genentech for providing the humanized anti-Her-2/*neu* monoclonal antibody Herceptin.

## REFERENCES

1. Weissleder R, Mahmood U. Molecular imaging. Radiology 2001;219: 316–333.
2. van Roessel P, Brand AH. Imaging into the future: visualizing gene expression and protein interactions with fluorescent proteins. Nat Cell Biol 2002;4:E15–20.
3. Yang M, Baranov E, Jiang P, Sun FX, Li XM, Li L, Hasegawa S, Bouvet M, Al-Tuwaijri M, Chishima T, Shimada H, Moossa AR, Penman S, Hoffman RM. Whole-body optical imaging of green fluorescent protein-expressing tumors and metastases. Proc Natl Acad Sci USA 2000;97: 1206–1211.
4. Contag PR, Olomu IN, Stevenson DK, Contag CH. Bioluminescent indicators in living mammals. Nat Med 1998;4:245–247.
5. Bulte JW, Zhang S, van Gelderen P, Herynek V, Jordan EK, Duncan ID, Frank JA. Neurotransplantation of magnetically labeled oligodendrocyte progenitors: magnetic resonance tracking of cell migration and myelination. Proc Natl Acad Sci USA 1999;96:15256–15261.
6. Weissleder R, Cheng HC, Bogdanova A, Bogdanov A Jr. Magnetically labeled cells can be detected by MR imaging. J Magn Reson Imag 1997;7:258–263.
7. Gohr-Rosenthal S, Schmitt-Willich H, Ebert W, Conrad J. The demonstration of human tumors on nude mice using gadolinium-labelled monoclonal antibodies for magnetic resonance imaging. Invest Radiol 1993;28:789–795.
8. Kobayashi H, Sato N, Kawamoto S, Saga T, Hiraga A, Haque TL, Ishimori T, Konishi J, Togashi K, Brechbiel MW. Comparison of the macromolecular MR contrast agents with ethylenediamine-core versus ammonia-core generation-6 polyamidoamine dendrimer. Bioconjug Chem 2001;12:100–107.
9. Sipkins DA, Cheresh DA, Kazemi MR, Nevin LM, Bednarski MD, Li KC. Detection of tumor angiogenesis in vivo by alphaVbeta3-targeted magnetic resonance imaging. Nat Med 1998;4:623–626.
10. Dodd SJ, Williams M, Suhan JP, Williams DS, Koretsky AP, Ho C. Detection of single mammalian cells by high-resolution magnetic resonance imaging. Biophys J 1999;76;103–109.
11. Kang HW, Josephson L, Petrovsky A, Weissleder R, Bogdanov A Jr. Magnetic resonance imaging of inducible E-selectin expression in human endothelial cell culture. Bioconjug Chem 2002;13;122–127.
12. Bulte JW, Hoekstra Y, Kamman RL, Magin RL, Webb AG, Briggs RW, Go KG, Hulstaert CE, Miltenyi S, The TH. Specific MR imaging of human lymphocytes by monoclonal antibody-guided dextran-magnetite particles. Magn Reson Med 1992;25:148–157.
13. Go KG, Bulte JW, de Ley L, The TH, Kamman RL, Hulstaert CE, Blaauw EH, Ma LD. Our approach towards developing a specific tumour-targeted MRI contrast agent for the brain. Eur J Radiol 1993;16:171–175.
14. Clarke C, Titley J, Davies S, O'Hare MJ. An immunomagnetic separation method using superparamagnetic (MACS) beads for large-scale purification of human mammary luminal and myoepithelial cells. Epithel Cell Biol 1994;3:38–46.
15. Venter DJ, Tuzi NL, Kumar S, Gullick WJ. Overexpression of the c-erbB-2 oncoprotein in human breast carcinomas: immunohistological assessment correlates with gene amplification. Lancet 1987;2:69–72.
16. Slamon DJ, Godolphin W, Jones LA, Holt JA, Wong SG, Keith DE, Levin WJ, Stuart SG, Udove J, Ullrich A, Press MF. Studies of the HER-2/neu proto-oncogene in human breast and ovarian cancer. Science 1989;244: 707–712.
17. DeGiovanna M. Clinical significance of HER-2/neu overexpression. Philadelphia: Lippincott Williams & Wilkins; 1999.
18. Wang SC, Zhang L, Hortobagyi GN, Hung MC. Targeting HER2: recent developments and future directions for breast cancer patients. Semin Oncol 2001;28:21–29.
19. Hnatowich DJ, Virzi F, Rusckowski M. Investigations of avidin and biotin for imaging applications. J Nucl Med 1987;28:1294–1302.
20. Shapiro HM. Practical flow cytometry. New York: Alan R. Liss; 1988.
21. Gullick WJ, Berger MS, Bennett PL, Rothbard JB, Waterfield MD. Expression of the c-erbB-2 protein in normal and transformed cells. Int J Cancer 1987;40:246–254.
22. Cremonesi M, Ferrari M, Chinol M, Stabin MG, Grana C, Prisco G, Robertson C, Tosi G, Paganelli G. Three-step radioimmunotherapy with yttrium-90 biotin: dosimetry and pharmacokinetics in cancer patients. Eur J Nucl Med 1999;26:110–120.
23. Koenig SH, Gillis P. Transverse relaxation (1/T2) of solvent protons induced by magnetized spheres and its relevance to contrast enhancement in MRI. Invest Radiol 1988;23 Suppl 1:S224–228.
24. Gillis P, Roch A, Brooks RA. Corrected equations for susceptibility-induced T2-shortening. J Magn Reson 1999;137:402–407.
25. Tanimoto A, Oshio K, Suematsu M, Pouliquen D, Stark DD. Relaxation effects of clustered particles. J Magn Reson Imag 2001;14:72–77.
26. Bremer C, Weissleder R. In vivo imaging of gene expression. Acad Radiol 2001;8:15–23.
27. Bryant LH Jr, Brechbiel MW, Wu C, Bulte JW, Herynek V, Frank JA. Synthesis and relaxometry of high-generation (G = 5, 7, 9, and 10) PAMAM dendrimer-DOTA-gadolinium chelates. J Magn Reson Imag 1999;9:348–352.
28. Sato N, Kobayashi H, Hiraga A, Saga T, Togashi K, Konishi J, Brechbiel MW. Pharmacokinetics and enhancement patterns of macromolecular MR contrast agents with various sizes of polyamidoamine dendrimer cores. Magn Reson Med 2001;46:1169–1173.